Singularities in weakly compressible flow through a porous medium

Yana Nec[1]

[1] Department of Mathematics and Statistics, Thompson Rivers University, British Columbia, Canada

E-mail: ynec@tru.ca

Abstract. The flow of weakly compressible fluid in an annular domain filled with a porous medium admits a wide class of solutions, whose axial symmetry is broken by azimuthally varying permeability. The structural parameters governing the underpinning dynamical system are the angles of sectors containing media of distinct permeability and values of the permeabilities themselves. Albeit from the vantage point of physics there is no apparent reason that certain configurations be singled out, mathematical analysis reveals an intriguingly complex pattern of singularities. The singular manifolds are loci, in whose vicinity saddle points of the underlying pressure field shift abruptly or appear / disappear. Stunningly the shift angle is independent of all configuration parameters, equalling $\pi/2$. When the system represents an injection or extraction well, the distance of the saddle points therefrom assumes the physical interpretation of the well's reach, also known as the radius of influence. Therefore two infinitesimally close configurations might have disparate flow fields and in particular zones of influence. This analysis casts in a new light the baffling difficulties encountered in the construction of aquifer sparging wells and landfill or natural gas collection wells, whose reach is known to be poorly predictable, and the failure or success of the injection / suction to induce the motion of adequate amounts of fluid proved moot. The traditional concept of the radius of influence is shown to be ill-posed and its unpredictability in practice intimately connected to the structural singularities of the anisotropic porous medium.

Keywords: anisotropic porous medium, exact flow solutions, zone of influence, singular manifold, high co-dimension

AMS classification scheme numbers: 37G10, 35Q35, 76E30, 76N10, 76S05

1. Introduction

The system studied herein is inspired by the problem of a weakly compressible flow through a porous medium filling an annular domain. The fluid is an ideal gas generated within the medium and obeying Darcy's law (Whitaker, 1986). Under steady conditions conservation of mass (Fulks et al., 1971) in conjunction with the ideal gas equation of state entails the following partial differential equation in polar coordinates (r,θ) with all quantities non-dimensional:

$$r\frac{\partial}{\partial r}\left(Kr\frac{\partial p^2}{\partial r}\right)+\frac{\partial}{\partial\theta}\left(K\frac{\partial p^2}{\partial\theta}\right)=-2r^2C, \qquad r_{\text{in}}<r<r_{\text{out}}, \quad 0<\theta<2\pi. \tag{1}$$

The parameters C and K stand for fluid generation rate and effective resistance due to matrix-fluid interaction respectively. r_{in} and r_{out} are the inner and outer radii of the annulus. The unknown p is the fluid pressure and thus must be a positive periodic function satisfying $p(r,\theta)=p(r,\theta+2\pi)$.

The domain is divided into N sectors of arbitrary angles. The contiguity rays θ_n, $n=\{1,\dots N\}$, are counted counter-clockwise and indexed so that θ_1 is the first one satisfying $\theta_1\geqslant 0$. Sector $n+1$ is bounded by rays θ_n and θ_{n+1} (consult figure 1). Both K and C are piecewise constant functions of θ, so that sector n is assigned values K_n and C_n such that $K_n\neq K_{n+1}$ and/or $C_n\neq C_{n+1}$ for any $1\leqslant n<N$, as well as $K_N\neq K_1$ and/or $C_N\neq C_1$. This final requirement of periodicity in a relationship of the type $(\,\cdot\,)_n=(\,\cdot\,)_{n+1}$ will be abbreviated hereinafter by indices $1\leqslant n\leqslant N$, tacitly implying the last index wraps back to 1.

It is desired to obtain a family of bounded solutions to (1), periodic in θ and in the C^0 continuity class with respect to the azimuthal derivative. Following the domain division, the solution $p(r,\theta)$ is a combination of N solutions $p_n(r,\theta)$ that are 2π-periodic and satisfy

$$r\frac{\partial}{\partial r}\left(r\frac{\partial p_n^2}{\partial r}\right)+\frac{\partial^2 p_n^2}{\partial\theta^2}=-2r^2C_n\Big/K_n, \quad 1\leqslant n\leqslant N, \qquad r_{\text{in}}<r<r_{\text{out}}; \quad \theta_{n-1}<\theta<\theta_n, \tag{2a}$$

$$p_n^2\Big|_{\theta_n^-}=p_{n+1}^2\Big|_{\theta_n^+}, \quad K_n\frac{\partial p_n^2}{\partial\theta}\bigg|_{\theta_n^-}=K_{n+1}\frac{\partial p_{n+1}^2}{\partial\theta}\bigg|_{\theta_n^+}. \tag{2b}$$

Equation (2b) ascertains that $p\in C^0$ and is obtained by integrating (1) over the domain $(\theta_n-\varepsilon,\theta_n+\varepsilon)$ and taking the limit $\varepsilon\longrightarrow 0$. In the physical world this condition conforms to continuity of azimuthal fluid velocity across the contiguity rays. The continuity of radial velocity follows from the smoothness of the pressure function in r. To complete the mathematical formulation of the problem, boundary conditions of either Dirichlet or Neumann-like type are set on the inner and outer circumference of the annulus:

$$p(\theta,r_{\text{in}})=p_{\text{in}}(\theta) \quad \text{or} \quad \frac{\partial p^2}{\partial r}\bigg|_{(r_{\text{in}},\theta)}=f_{\text{in}}(\theta); \qquad \text{and}$$

$$p(\theta,r_{\text{out}})=p_{\text{out}}(\theta) \quad \text{or} \quad \frac{\partial p^2}{\partial r}\bigg|_{(r_{\text{out}},\theta)}=f_{\text{out}}(\theta). \tag{2c}$$

The form of the Neumann condition is somewhat unconventional, however quite natural for this system, since the functions f_{in} and f_{out} are directly convertible to fluid flux normal to the boundary.

As is shown hereunder, this system is mathematically unique due to a plethora of singularities harboured by (2) and the concomitant structural discontinuities within this family of solutions bearing on the physical interpretation of (2) as a flow field and in particular its stagnation points. In several environmental engineering applications this translates to the ability of a well to inject fluid into a porous medium or draw it therefrom. Conventionally the zone of influence is assumed to be axially symmetric despite evidence to the contrary, and characterised by a single scalar, referred to as the radius of influence. The inadequacy of this description for a compressible fluid was recognised as

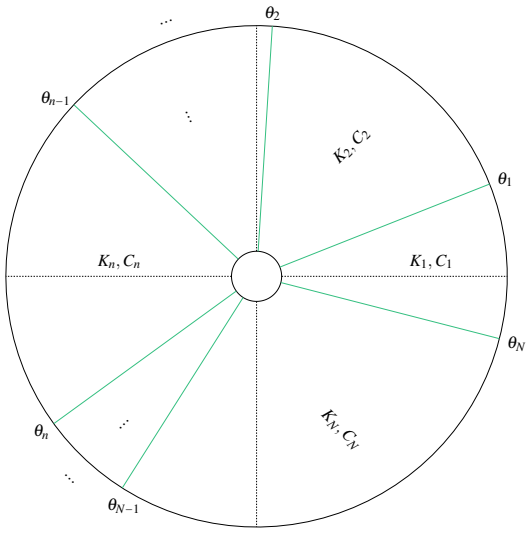

Figure 1. Flow domain schematic: indexing of contiguity rays θ_n and intrinsic matrix properties K_n, C_n, $1 \leqslant n \leqslant N$

early as 1960s, e.g. Al-Hussainy et al. (1966) proposed a sophisticated compressibility modelling in an axisymmetric geometry via a pseudo-pressure variable. Studies without the assumption of axial symmetry exist, but are rare and do not focus on the zone of influence. Some examples are Young (1989), where isobars within a cross-section plane of an arbitrary set of vertical landfill wells demonstrate the asymmetric flow field; and Freedman et al. (2013), where the fluid is incompressible and hydraulic pressure contours are shown to break azimuthal symmetry. A distinct type of work pursues the identification of preferential flow directions based on the structure of the porous matrix (Mauran et al., 2001; Li, Lu, Luo, Sun, Shen, Hu, Liu, Qi, Guan and Guo, 2019). The relation between the local morphology of the porous matrix and its global resistance to flow is often explored in artificially generated media with no immediate connexion to wells (Germanou et al., 2018; Li, Ki, Jing, Xiao and Cui, 2019). A well's zone of influence embodies the conceptual intersection between the functionality of the localised engineering facility and response of its geographically extensive natural surroundings, both vying for control. Wheresoever the structure of the circumambient matrix is uncertain, operators face baffling phenomena and moot success. Advanced techniques in geological imaging usually improve the outcome, and are a topic of active research (Mair et al., 1999), but are often expensive and not universally applicable.

In contaminated aquifer remediation via air injection into the surrounding medium the sparging well radius of influence is difficult to estimate in part due to differences in the permeability of saturated and unsaturated zones (Lundegard and LaBrecque, 1995). Field studies traditionally report concentration of oxygen, helium, carbon dioxide and contaminants versus radial distance and depth of monitoring points (Agarwal et al., 2005; Lundegard and LaBrecque, 1995), omitting their azimuthal location. Nevertheless the argument applies equally thereto, as it stands to reason the soil is unlikely to be azimuthally isotropic whilst manifesting conspicuous anisotropy in other directions.

In natural gas development advanced modelling of fluid propagation in selected directions evinces the need to seek descriptions beyond axial symmetry (Hyman et al., 2015). The landfill gas industry also struggles to define the radius of influence, the evidence ranging from inventions targeting the modification of permeability properties of subsurface strata at selected spots in the vicinity of landfills, yet outside their nominal perimeter (Stenborg and Williams, 1994); and to contention of estimates via disparate approaches in order to improve the long-standing poor predictability of this quantity (Vigneault et al., 2004). The exerted suction might have a significant (Kutsyi, 2015) or minimal (figure 3 of Nec and Huculak (2019)) impact on the radius of influence, or equivalently the mass extracted. Thus it is not surprising that the apparent radius of influence cannot be used as a basis for illative parameters (Walter,

2003). All foregoing types of wells have been constructed and operated for many decades. Accumulated experience notwithstanding, each new site seems to defy quondam models, qualitative and quantitative alike.

In essence any well's reach depends on the effective matrix resistance to flow. The abundance of evidence of the medium heterogeneity in conjunction with the paucity of literature examining azimuthal variation suggests dearth of means rather than lack of interest. A recent study reported a wide closed form class of flow solutions with azimuthally varying permeability (Nec and Huculak, 2020). A comprehensive chronological survey of analytical flow solutions in anisotropic porous media can be found therein. The classical notion of the radius of influence becomes a generalised entity in the form of a set of stagnation points and separatrix contours joining them. Whist this class of flow fields opens the possibility of modelling unencumbered by axial symmetry and more realistic estimates of the radius of influence, it harbours a dismayingly extensive pattern of structural singularities. The current contribution provides a complete analysis substantiating the difficulties encountered in effective operation of the aforementioned engineering facilities and in experimental studies documenting the zones of influence thereof. This is the first analytical demonstration that reconciles decades of inconsistent measurements and numerous approaches attempting to model deterministically a quantity so elusive as to behave almost as a random variable. Given that it is not in fact random, the only sound explanation of such sensitivity is in the existence of strong underlying singularities occurring frequently enough to throw out of kilter any individual attempt to obtain a reliable description.

This study constructs a mathematical argument that conclusively proves the apparent labile dependence of the zone of influence on local matrix properties is intrinsic to the weakly compressible flow through anisotropic porous media and thus inevitable. Two interlaced points pertain to the engineering applications employing this type of flow. One, the notion that the zone of influence of a gas well is circular, adopted from the traditional hydraulic well modelling, is ill grounded. A revised concept natural in the context of compressible fluids is suggested instead. Two, the erratic data recordings of fluid pressure and velocity, or solute concentration around a gas well are not to be ascribed to the instrumentation used. The analysis herein implies the fluctuations are a physical attribute of the flow field and sets the framework to fathom the flow behaviour in a specific site. Collection of data on the azimuthal variation of permeability around the well and accurate tracking of ranges thereof over periods of time relevant to the lifetime of the facility, for instance seasonal or in the case of a landfill related to the characteristic waste degradation time, are essential steps. Such data will allow to predict the respective variability in the well's reach along with regions of fluid circulation or escape, and thus optimise the efficiency of operation. Most importantly, when the problematic locales are identified, the suggested theory further allows to predict where possible efforts to modify the medium permeability (such as hydraulic fracturing or landfill waste compacting) should be focussed in order to attain adequate flow in all azimuthal directions.

§2 contains the mathematical analysis and is structured as follows. Theorem 1 derives the solution to system (2), proves it is singular on a certain manifold within the parameter space, and calculates the dimension of the manifold. §2.1 shows that in the case of two sectors the manifold is a straight line, whereupon lemma 1 proves that any stagnation point in the flow must be a saddle point and establishes the abrupt shift by an angle of $\pi/2$ observed in infinitesimally close configurations on two sides of the line. Figure 2 depicts an example of such an occurrence. Observe the two flow fields are starkly different despite nearly identical geometry. §2.2 determines that the singular manifold for the case of three sectors comprises a set of petal-shaped orbits replicated periodically in the $\{\theta_1, \theta_2\}$ space. Proposition 1 characterises the regularity corridors, i.e. the parts of the parameter space, where no such orbit is encountered. These are crucial in estimating the likelihood an arbitrarily chosen configuration is proximate to a singular one and thus prone to manifest strong changes in the flow pattern in response to small changes in the geometry. Whilst the probability that any one given configuration happens to be singular is minuscule, the narrowness of the corridors means the probability to fall *near* a singularity is quite high, especially when the matrix is characterised by permeabilities spanning several orders of magnitude or a large number of sectors, both implying the existence of preferential flow directions. §2.3 obtains the explicit expression for the singular manifold in the case of four sectors – the highest number that is feasible to solve analytically, and shows that the periodic structure of petal-shaped surfaces persists, whilst the part of the space free therefrom becomes much more difficult to delineate, implying that as the number of sectors increases, so does the likelihood of proximity to a singular configuration and concomitant sensitivity to geometry changes. Theorem 2 in §2.4 extends lemma 1 to a configuration comprising any number of sectors and thus conclusively explains the inconsistent well flow behaviour observed in the field.

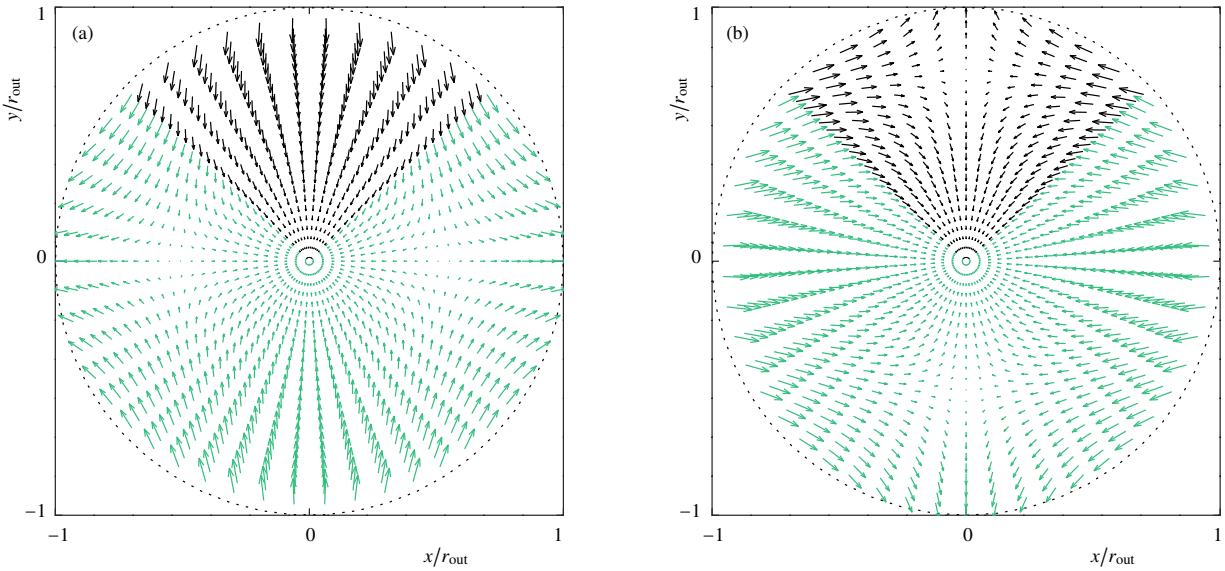

Figure 2. Example of near singular configurations: close geometry, yet disparate velocity fields. (a) $\theta_1 = \pi/4 + \varepsilon$, $\theta_2 = 3\pi/4 - \varepsilon$. (b) $\theta_1 = \pi/4 - \varepsilon$, $\theta_2 = 3\pi/4 + \varepsilon$. Common parameters: $\varepsilon = 0.01\pi$ and $K_1/K_2 = 0.5$.

2. Steady flow singularity

Herein a minor formal restriction on the division of the annulus into sectors is required. Suppose that there exists an angle $\theta_o = \pi/n_o$ for some integer $n_o \in \mathbb{N}$, such that each contiguity ray θ_n satisfies $\theta_n = \tilde{n}_n \theta_o$ for some integer $\tilde{n}_n \in \mathbb{N}$. In other words, all sectors are rational multiples $\tilde{n}_n/n_o$ of π and $\sum_{n=1}^{N} \left(\tilde{n}_{n+1} - \tilde{n}_n\right) \Big/ n_o = 2$, where $\tilde{n}_{N+1}$ corresponds to the ray $\theta_1 + 2\pi$. Since the set of rational numbers $\mathbb{Q}$ is dense within the set of real numbers $\mathbb{R}$, this restriction, albeit possibly inconvenient, is but a formality. Such a division of the annulus will be referred to as a rational division. The following theorem delineates the existence of a steady flow solution and attendant structural singularity.

Theorem 1. *Suppose the contiguity rays θ_n conform to a rational division with a base sector $\theta_o = \pi/n_o$, and $K_n \neq K_{n+1}$, $1 \leqslant n \leqslant N$. Let $p_{bc}(\theta)$ and/or $f_{bc}(\theta)$ be integrable functions containing at least one of* $\sin(2\theta_n)$, $\cos(2\theta_n)$ *harmonics and possibly other harmonics of frequencies $\tilde{m}n_o$, $\tilde{m} \geqslant 0$ integer, and the subscript $(\,\cdot\,)_{bc}$ standing for both $(\,\cdot\,)_{in}$ and $(\,\cdot\,)_{out}$, prescribing boundary conditions (2c) on the inner and outer arcs of one given sector. Then system (2) possesses a unique solution bar on a singular manifold independent of the harmonics $\tilde{m}n_o \neq 2$ and of dimension $2(N-1)$ at most within the parameter space $\{\theta_n, K_n, C_n\}_{n=1}^{N}$.*

Proof. System (2) is solvable by the separation of variables technique. Define functions P_n via

$$p_n^2 = P_n(r,\theta) - \frac{C_n}{2K_n} r^2 \tag{3}$$

and separate $P_n = A_n(r)B_n(\theta)$ to obtain

$$r\Big(rA'\Big)' - \alpha^2 A = 0, \qquad B'' + \alpha^2 B = 0, \tag{4}$$

where α is a suitable constant, generally complex. Since P_n must be periodic in θ and bounded, $\alpha \in \mathbb{R}$. The space of solutions to (4) is

$$A(r) = \operatorname{span}\Big\{r^{\alpha}, r^{-\alpha}\Big\}, \quad B(\theta) = \operatorname{span}\Big\{\sin(\alpha\theta), \cos(\alpha\theta)\Big\}, \qquad \alpha > 0 \tag{5a}$$

$$A(r) = \operatorname{span}\left\{1, \ln r\right\}, \quad B(\theta) = \operatorname{span}\left\{1, \theta\right\}, \qquad \alpha = 0. \tag{5b}$$

The case $\alpha < 0$ introduces a dependent basis and thus requires no more attention. The periodicity requirement yields the set $\{\alpha = m \mid m \in \mathbb{N}\}$. Discarding the solution $B(\theta) = \theta$, the most general acceptable solution is of the form

$$p_n^2 = \frac{C_n}{2K_n}\left\{ -r^2 + b1_0^{(n)} + b2_0^{(n)} \ln r + \sum_{m=1}^{\infty}\left(\left(a1_m^{(n)} r^m + a2_m^{(n)} r^{-m}\right)\sin(m\theta) + \left(b1_m^{(n)} r^m + b2_m^{(n)} r^{-m}\right)\cos(m\theta)\right)\right\}. \tag{6}$$

Subject to a rational division, equations (2b) lead to the following distinction. There exists a subset $m = \tilde{m}n_o$, $\tilde{m} \geqslant 0$ an integer, such that $\sin(m\theta_n) = 0$ for all $1 \leqslant n \leqslant N$, whereas $\cos(m\theta_n) \neq 0$. If this subset contains $m = 2$, it is to be excluded and treated separately. For $m \neq \tilde{m}n_o$ neither $\sin(m\theta_n)$ nor $\cos(m\theta_n)$ vanishes. Thus for $m \geqslant 1$, $m \neq \tilde{m}n_o$, equation (2b) yields

$$\begin{pmatrix} C_n \big/ K_n & -C_{n+1} \big/ K_{n+1} \\ C_n & -C_{n+1} \end{pmatrix} \mathbf{c} = \begin{pmatrix} 0 \\ 0 \end{pmatrix}, \quad i = \{1,2\}, \tag{7a}$$

where the vector $\mathbf{c}$ equals

$$\begin{pmatrix} b_{im}^{(n)} \\ b_{im}^{(n+1)} \end{pmatrix} \quad \text{or} \quad \begin{pmatrix} a_{im}^{(n)} \\ a_{im}^{(n+1)} \end{pmatrix}, \quad i = \{1,2\}.$$

Since $K_n \neq K_{n+1}$, a trivial solution follows. For $m = \tilde{m}n_o$ one of the equations in (2b) is satisfied automatically by the construction of the rational division, whence

$$\frac{C_n}{K_n} b_{im}^{(n)} = \frac{C_{n+1}}{K_{n+1}} b_{im}^{(n+1)}, \quad C_n a_{im}^{(n)} = C_{n+1} a_{im}^{(n+1)}, \tag{7b}$$

both of which are degenerate $N \times N$ systems with a single degree of freedom. In the case of the coefficients $b_{im}^{(n)}$, the above also holds for $m = 0$ and thus completes the treatment of the terms corresponding to the pair $\{1, \ln r\}$. For $m = 2$ and $i = 2$ the foregoing analysis stands. For $m = 2$ and $i = 1$ equations (2b) give the linear system

$$\mathfrak{C}\mathbf{c} = \mathbf{r}, \tag{7c}$$

wherein the matrix $\mathfrak{C}$ is almost block bi-diagonal

$$\mathfrak{C} = \begin{pmatrix} \mathfrak{A}_1 & \mathfrak{B}_1 & & & \\ & \mathfrak{A}_2 & \mathfrak{B}_2 & & \\ & & \ddots & \ddots & \\ & & & \mathfrak{A}_{N-1} & \mathfrak{B}_{N-1} \\ \mathfrak{B}_N & & & & \mathfrak{A}_N \end{pmatrix},$$

comprising the blocks

$$\mathfrak{A}_n = \begin{pmatrix} \sin(2\theta_n) & \cos(2\theta_n) \\ \cos(2\theta_n) & -\sin(2\theta_n) \end{pmatrix}, \qquad \mathfrak{B}_n = \begin{pmatrix} -k_n \sin(2\theta_n) & -k_n \cos(2\theta_n) \\ -c_n \cos(2\theta_n) & c_n \sin(2\theta_n) \end{pmatrix}$$

with $c_n = C_{n+1} \big/ C_n$ and $k_n = c_n K_n \big/ K_{n+1}$. The unknown vector $\mathbf{c}$ and right-hand side vector $\mathbf{r}$ equal respectively

$$\mathbf{c} = \left(a1_2^{(1)} \; b1_2^{(1)} \quad \cdots \quad \cdots \quad a1_2^{(N)} \; b1_2^{(N)}\right)^{\mathrm{T}} \qquad \text{and} \qquad \mathbf{r} = \left(1 - k_1 \quad 0 \quad \cdots \quad \cdots \quad 1 - k_N \quad 0\right)^{\mathrm{T}}.$$

The non-zero right-hand side vector $\mathbf{r}$ implies that the $m = 2$ harmonics are essential for the existence of the steady state solution.

The degrees of freedom endowed by (7b) allow for boundary conditions of any combination from (2c) to be imposed on the inner and outer arcs of one sector. Let its index be n_*. The boundary conditions on the complementary arcs follow by the solution of (7b). Consider the inner product

$$< f_1, f_2 >= \int_I f_1(\theta) f_2(\theta) \mathrm{d}\theta, \tag{8}$$

where $f_i(\theta)$ are integrable functions, $i = \{1,2\}$. The interval I might be the standard choice $[-\pi,\ \pi]$, or if it is preferable to begin the integration from the contiguity ray of the sector n_*, I should be taken as $[\theta_{n_*},\ \theta_{n_*}+4\pi]$. In the latter case due to the arbitrary starting point θ_{n_*} it is necessary to double the interval length in order to ensure orthogonality within the basis $\{\cos(m\theta), \sin(m\theta)\}$. The conventional product over the interval $[-\pi,\ \pi]$ relies on the π-periodicity of the sine function roots, but the fact that $\sin(\pi m) = 0$ for all integer m ceases being useful when $\theta_{n_*} \neq -\pi$. Instead one must invoke the full 2π period of the sine and cosine functions. Note that albeit p_n corresponds to the physical flow field within one sector only, mathematically the function is defined in the entire annulus, enabling the use of (8) identically for all n. The boundary conditions for the chosen sector n_* must be similarly extended. With this product for any $\tilde{m} \geqslant 1$, $m = \tilde{m} n_o$, the following equation ensues for the coefficients $b_{im}^{(n_*)}$:

$$r_{\mathrm{bc}}^{m} b_{1m}^{(n_*)} + r_{\mathrm{bc}}^{-m} b_{2m}^{(n_*)} = \frac{K_{n_*}}{\pi C_{n_*}} \int_{\theta_{n_*}}^{\theta_{n_*}+4\pi} p_{\mathrm{bc}}^2(\theta) \cos(m\theta) \mathrm{d}\theta \tag{9a}$$

if the desired condition is of the Dirichlet type, and

$$r_{\mathrm{bc}}^{m-1} b_{1m}^{(n_*)} - r_{\mathrm{bc}}^{-m-1} b_{2m}^{(n_*)} = \frac{K_{n_*}}{\pi m C_{n_*}} \int_{\theta_{n_*}}^{\theta_{n_*}+4\pi} f_{\mathrm{bc}}(\theta) \cos(m\theta) \mathrm{d}\theta \tag{9b}$$

for the Neumann-like condition. The subscript $(\ \cdot\ )_{\mathrm{bc}}$ stands for $(\ \cdot\ )_{\mathrm{in}}$ or $(\ \cdot\ )_{\mathrm{out}}$ as needed. Thus for all four combinations of Dirichlet and Neumann-like conditions a 2×2 linear non-degenerate system yields $b_{im}^{(n_*)}$, $i = \{1,2\}$. A simple replacement of $\cos(m\theta)$ by $\sin(m\theta)$ gives the respective $a_{im}^{(n_*)}$. For $m = 0$

$$b_{10}^{(n_*)} + \ln r_{\mathrm{bc}}\, b_{20}^{(n_*)} = \frac{K_{n_*}}{2\pi C_{n_*}} \int_{\theta_{n_*}}^{\theta_{n_*}+4\pi} p_{\mathrm{bc}}^2(\theta) \mathrm{d}\theta + r_{\mathrm{bc}}^2 \tag{9c}$$

or

$$\frac{b_{20}^{(n_*)}}{r_{\mathrm{bc}}} = \frac{K_{n_*}}{2\pi C_{n_*}} \int_{\theta_{n_*}}^{\theta_{n_*}+4\pi} f_{\mathrm{bc}}(\theta) \mathrm{d}\theta + 2 r_{\mathrm{bc}}. \tag{9d}$$

Again, for any of the four possible Dirichlet and Neumann-like combinations the system is non-degenerate. Therefore by (9) no boundary condition can introduce a singularity into the flow field (2), and the sole source thereof is $\det \mathfrak{C}$. Thus if $\det \mathfrak{C} \neq 0$, the existence of the steady state is established. It must be unique by the linearity of system (2) in p_n^2.

To establish the dimension of the singular manifold defined by $\det \mathfrak{C} = 0$, observe that in (7b) it is possible to map

$$\begin{pmatrix} a_{im}^{(n)} \\ b_{im}^{(n)} \end{pmatrix} \longmapsto C_n \begin{pmatrix} a_{im}^{(n)} \\ b_{im}^{(n)} \end{pmatrix},$$

whereby $\mathfrak{C}$ no longer depends on c_n. Thus its determinant involves at most $2N$ arguments: $\{\theta_n, k_n\}_{n=1}^{N}$. Hence for the current purpose it is possible to set $c_n = 1\ \forall 1 \leqslant n \leqslant N$. Since

$$k_1 \cdot \cdots \cdot k_N = \frac{K_1}{K_2} \cdots \frac{K_{N-1}}{K_N} \frac{K_N}{K_1} = 1,$$

out of N ratios only $N-1$ are independent parameters. Therefore $\det \mathfrak{C}$ is a function of $2N-1$ arguments, and the manifold $\det \mathfrak{C} = 0$ is of dimension $2(N-1)$ at most. □

Corollary 1. *The singular manifold* $\det\mathfrak{C}=0$ *is* $\pi/2$ *periodic in* θ_n, $1\leqslant n\leqslant N$.

Proof. The entries of the matrix $\mathfrak{C}$ contain $\sin(2\theta_n)$ and $\cos(2\theta_n)$. Inspect how a shift of $\pi\tau/2$ with $0<\tau\leqslant 1$ affects these terms:

$$\sin\big(2(\theta_n+\pi\tau/2)\big)=\sin(2\theta_n)\cos(\pi\tau)+\cos(2\theta_n)\sin(\pi\tau),$$
$$\cos\big(2(\theta_n+\pi\tau/2)\big)=\cos(2\theta_n)\cos(\pi\tau)-\sin(2\theta_n)\sin(\pi\tau).$$

Therefore the minimal value of τ is $\tau=1$, whereby the mapping $\theta_n\longmapsto\theta_n+\pi/2$ causes all entries of $\mathfrak{C}$ to reverse their sign. Since the size of the matrix is $2N\times 2N$, $\det\mathfrak{C}$ is invariant under this mapping. □

The main part of this study is dedicated to gleaning the properties of the singular manifold $\det\mathfrak{C}=0$, as they determine the extent of encumbrance imposed upon the flow field (2), or from a different point of view, the robustness and controllability of (2) as a dynamical system. The fact that the dimension of this manifold is N-dependent, is a harbinger of a singularity that is easy to encounter in a practical setting. Since the manifold is given in an implicit form, begin by the illustration of particular cases with low N.

2.1. $N=2$

For two sectors $\mathfrak{C}$ is a full 4×4 matrix. Appealing to the technique of Schur complement, $\mathfrak{C}$ is multiplied on the right by $\begin{pmatrix}\mathrm{I}_{2\times 2} & 0_{2\times 2}\\ -\mathfrak{A}_2^{-1}\mathfrak{B}_2 & \mathrm{I}_{2\times 2}\end{pmatrix}$, whereby the computation of $\det\mathfrak{C}$ reduces to that of a 2×2 matrix, since the determinant of the foregoing auxiliary matrix equals unity. Upon simplification $\det\mathfrak{C}=0$ results in

$$\cos\big(4(\theta_2-\theta_1)\big)=1, \tag{10}$$

and thence the candidate manifolds are $\theta_2-\theta_1=\pi/2$ and $\theta_2-\theta_1=\pi$. Upon a closer scrutiny it becomes apparent that the latter is not a true singularity: equations (2b) on the ray θ_2 enforce nought but periodicity and so are superfluous. The remaining two equations on the ray θ_1 do possess a unique solution. By contrast, the manifold $\theta_2-\theta_1=\pi/2$ is truly singular. Its dimension is only 1. In this case of the minimal number of sectors the ratios k_n do not figure altogether. This degeneracy does not occur for $N>2$. The $\pi/2$ periodicity by corollary 1 is also degenerate in this case. Therefore any configuration with a sector of a right angle and arbitrary permeabilities possesses no steady state solution. Since physical systems do not support mathematical singularities, the dynamics in the proximity of the singular manifold might evince abrupt transitions and possibly chaotic behaviour. The analysis below establishes that herein the nature of the singularity begets a sudden shift of the flow field's stagnation points. From the fluid dynamics perspective such a shift means that exactly at the singular configuration no steady state exists, whilst in its vicinity the pressure contours and hence streamlines must rearrange abruptly upon an infinitesimal change in the sector angles. This explains the high uncertainty of the flow behaviour experienced in the field. The example for $N=2$ allows to trace this mechanism with relative ease before generalising the proof to an arbitrary configuration.

Since $N=2$, a symmetry line bisects both sectors. As (1) is invariant with respect to translation in θ, it suffices to consider just one orientation of this symmetry line, for instance the vertical. Then $a_{1\,2}^{(n)}=0$, $n=\{1,2\}$. The singular configuration is $\theta_1=\pi/4$ and $\theta_2=3\pi/4$. The following lemma delineates the dynamics in the vicinity thereof. Arbitrary respective deviations ε_1 and ε_2 require centring, whereupon the configuration must be rotated to keep the symmetry line vertical, resulting in anti-symmetric deviations $\varepsilon_1=-\varepsilon_2\overset{\text{def}}{=}\varepsilon$.

Lemma 1. *Let* $N=2$ *and without loss of generality*

$$p_n^2=\frac{C_n}{2K_n}\left\{b_{1\,0}^{(n)}+b_{2\,0}^{(n)}\ln r+r^2\Big(-1+a_{1\,2}^{(n)}\sin(2\theta)+b_{1\,2}^{(n)}\cos(2\theta)\Big)\right\}$$

be the solution (6) containing no harmonics with $m>2$. *Further let* $\theta_1=\pi/4+\varepsilon$ *and* $\theta_2=3\pi/4-\varepsilon$, $|\varepsilon|\ll 1$. *Then*
(i) if critical points exist, they are saddle points located on the horizontal or vertical;
(ii) when ε *changes sign, said saddle points abruptly shift from the horizontal to vertical or vice versa.*

Proof. System (7c) yields

$$a_{1\,2}^{(n)} = 0, \quad b_{1\,2}^{(n)} = -\sec(2\varepsilon), \quad n = \{1,2\}. \tag{11}$$

The derivative $\dfrac{\partial p}{\partial \theta}$ is discontinuous on the contiguity rays. Therefore the critical points can only lie in a sector interior, and henceforth in this proof the sector index is omitted to avoid notation cumbersomeness. Seeking possible critical points (r_*, θ_*) in either sector by solving $\nabla p = \mathbf{0}$ yields

$$\frac{b_{20}}{r_*} + 2r_*\Big(-1 + b_{12}\cos(2\theta_*)\Big) = 0, \tag{12a}$$

$$b_{12}\sin(2\theta_*) = 0. \tag{12b}$$

As $b_{12} \neq 0$, by (12b) it follows that θ_* assumes the values $\theta_* = \{0, \pi\}$ or $\theta_* = \{\pi/2, 3\pi/2\}$, bearing in mind that symmetry across the vertical must be maintained. Thus if critical points exist, they must lie either on the horizontal or vertical. Equation (12a) gives

$$2r_*^2 = \frac{b_{20}}{1 + \cos(2\theta_*)\sec(2\varepsilon)} \sim b_{20}\frac{\sin(2\varepsilon)}{\cos(2\theta_*)},$$

where the asymptotic relation follows by $|\varepsilon| \ll 1$. The right-hand side must be positive. The coefficient b_{20} is fixed given specific boundary conditions. Therefore if ε changes sign, $\cos(2\theta_*)$ must follow suit. This is accorded by θ_* "skipping" from the horizontal to vertical or vice versa.

It remains only to show that (r_*, θ_*) are indeed saddle points. To this end it is easier to write the solution in Cartesian coordinates (the points' location or type is not affected by the choice of coordinates) and temporarily set $C/(2K) = 1$, since a positive scalar factor cannot affect the nature of the critical point. Thus

$$p^2 = b_{10} + \frac{b_{20}}{2}\ln\big(x^2 + y^2\big) + 2a_{12}xy + \big(b_{12} - 1\big)x^2 - \big(b_{12} + 1\big)y^2.$$

It is necessary to show that the determinant of the Hessian matrix $p_{xx}p_{yy} - p_{xy}^2 < 0$, and in particular $p_{xx}p_{yy} < 0$ suffices. Evaluation of these second order derivatives for θ_* on the horizontal, using $b_{20}/r_*^2 = 2\big(1 - b_{12}\big)$, gives

$$p_{xx} = \frac{2}{p}\big(b_{12} - 1\big), \quad p_{yy} = -\frac{2}{p}b_{12},$$

so that

$$p_{xx}p_{yy} = -\frac{4}{p^2}\sec(2\varepsilon)\big(\sec(2\varepsilon) + 1\big) \sim -\frac{4}{p^2}\sec^2(2\varepsilon) < 0,$$

where $|\varepsilon| \ll 1$ was used. Similarly for θ_* on the vertical $b_{20}/r_*^2 = 2\big(1 + b_{12}\big)$ and

$$p_{xx} = \frac{2}{p}b_{12}, \quad p_{yy} = -\frac{2}{p}\big(b_{12} + 1\big),$$

giving

$$p_{xx}p_{yy} = -\frac{4}{p^2}\sec(2\varepsilon)\big(\sec(2\varepsilon - 1)\big) \sim -\frac{4}{p^2}\sec^2(2\varepsilon) < 0.$$

□

Figure 3 illustrates this phenomenon: in configurations comprising nearly right-angled sectors the stagnation points abruptly shift from the line bisecting the two sectors to its perpendicular or vice versa. Note that in doing so, the two points in the bottom sector in figure 3(a) are replaced by a single point situated at the same distance from the well, whereas the new point in the top sector in figure 3(b) is much farther. Translating this to a practical situation, suppose roughly a quarter of the medium to the north of a sparging or gas extraction well is of a distinct permeability.

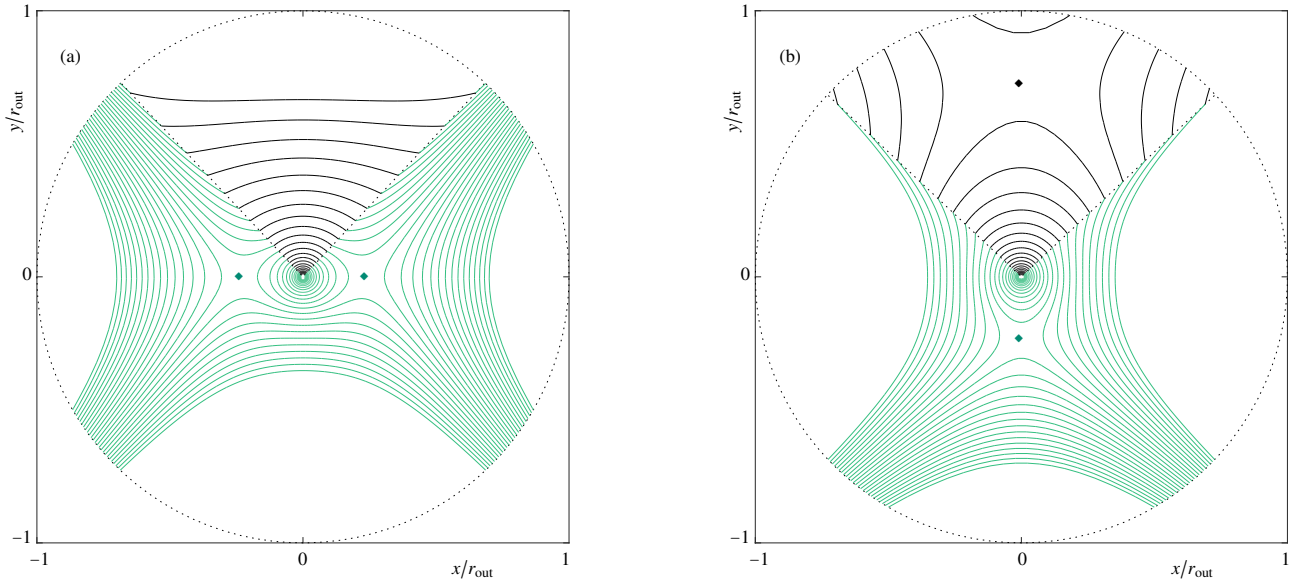

Figure 3. Pressure contours for configuration of lemma 1 with $\varepsilon = 0.01\pi$ and $k_1 = 0.1$. Diamonds mark saddle points. Note that the saddle points lie on the horizontal in (a) and on the vertical in (b).

In the complementary sector – green / grey contours in figure 3(a) – the zone of influence is delimited by the largest closed contour. Since traditional measurements assume a radius, i.e. a single scalar, the contour's notably oblate shape will result in a rather large discrepancy between monitoring points in the south versus east / west, in this example about a factor of 2. Yet neither will be found consistent when juxtaposed with the virtually infinite radius of influence suggested by monitoring points in the northern sector. Moreover, if in the course of a few weeks that sector shrinks somewhat (e.g. due to changes in saturation) and the measurements are taken again, the readings at the southern and eastern / western points will swap, whereas the formerly infinite northern one will suddenly become commensurate with the rest. This kind of uncertainty is well familiar to field personnel monitoring the wells, and collected data are wontedly cleaned heavily before becoming remotely presentable. This analysis suggests the inability to collect consistent measurements, often blamed on instrumentation as well as external factors, is in fact an intrinsic property of this type of flow. This behaviour is not unique to the configuration of two right-angled sectors and is further developed hereunder.

2.2. N = 3

For N=3 the matrix $\mathfrak{C}$ in (7c) has the form

$$\mathfrak{C} = \begin{pmatrix} \mathfrak{A}_1 & \mathfrak{B}_1 & \\ & \mathfrak{A}_2 & \mathfrak{B}_2 \\ \mathfrak{B}_3 & & \mathfrak{A}_3 \end{pmatrix}. \tag{13}$$

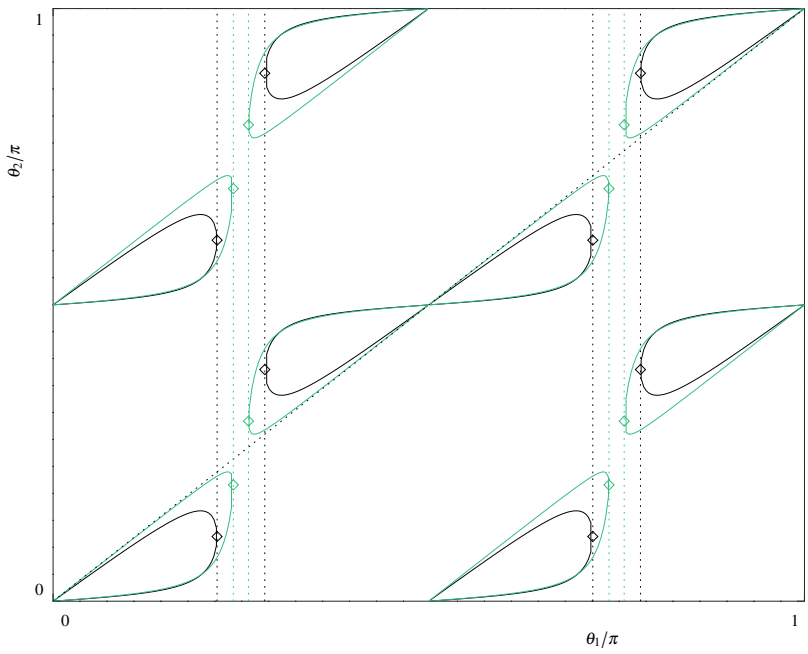

Figure 4. Singular manifold $\theta_2(\theta_1)$ by (15) with $k_1 = 0.1$, $k_2 = 100$ (black) and $k_1 = 0.01$, $k_2 = 1000$ (green / grey). Dotted vertical lines show the respective regularity corridors determined by equation (19) and geometrically corresponding to the tangency points with the petal-shaped contours (marked by diamonds). The diagonal dotted line delimits the restriction $\theta_1 < \theta_2$. Figure 6 gives corresponding $f(\theta_1)$, equation (16a)

Due to the rotational invariance of (1) it is possible to take $\theta_3 = 2\pi$ without loss of generality. Mutiplying $\mathfrak{C}$ on the right by $\begin{pmatrix} \mathrm{I}_{2\times2} & 0_{2\times2} & 0_{2\times2} \\ 0_{2\times2} & \mathrm{I}_{2\times2} & 0_{2\times2} \\ -\mathfrak{A}_3^{-1}\mathfrak{B}_3 & 0_{2\times2} & \mathrm{I}_{2\times2} \end{pmatrix}$, it becomes evident that $\det\mathfrak{C} = 0$ if and only if

$$\det\begin{pmatrix} \mathfrak{A}_1 & \mathfrak{B}_1 \\ \widetilde{\mathfrak{B}}_2 & \mathfrak{A}_2 \end{pmatrix} = 0, \tag{14}$$

wherein the bottom left block $\widetilde{\mathfrak{B}}_2$ is given by

$$\widetilde{\mathfrak{B}}_2 = \begin{pmatrix} -k_2c_3\sin(2\theta_2) & -k_2k_3\cos(2\theta_2) \\ -c_2c_3\cos(2\theta_2) & k_3c_2\sin(2\theta_2) \end{pmatrix}$$

with c_n and k_n as defined beneath (7c). Computing this determinant, using trigonometric identities as well as simplifying the products of the different combinations of c_n and k_n (all dependence on C_n disappears as expected), gives

$$\cos(4\theta_1)\left\{\tilde{k}_{12}+\tilde{k}_{13}-\tilde{k}_{23}-2\right\}+\cos(4\theta_2)\left\{-\tilde{k}_{12}+\tilde{k}_{13}+\tilde{k}_{23}-2\right\}+\cos\big(4(\theta_2-\theta_1)\big)\left\{\tilde{k}_{12}-\tilde{k}_{13}+\tilde{k}_{23}-2\right\}=\tilde{k}_{12}+\tilde{k}_{13}+\tilde{k}_{23}-6, \tag{15a}$$

where

$$\tilde{k}_{ij} = \frac{K_i}{K_j} + \frac{K_j}{K_i}. \tag{15b}$$

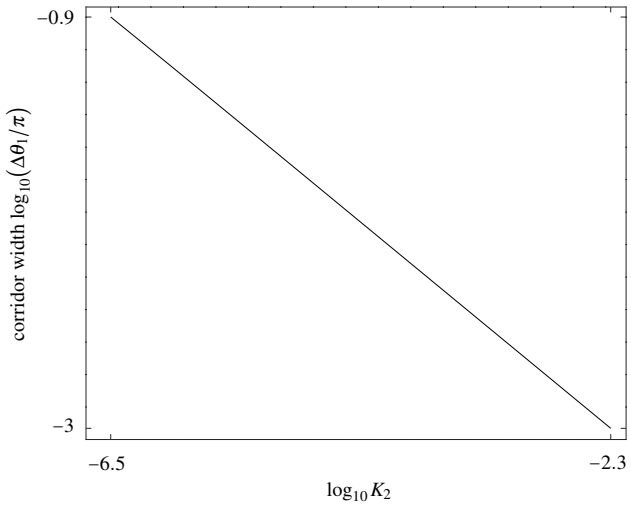

Figure 5. Dependence of regularity corridors $\Delta\theta_1$ on permeability of one sector. $K_1 = 10^{-7}$, $K_3 = 10^{-8}$.

Note that (15) is periodic with the requisite period $\pi/2$ in both θ_1 and θ_2. Bearing in mind the fixed ray θ_3, this corresponds to a 4-dimensional manifold in the space $\{\theta_n\}_{n=1}^{3} \bigcup \{k_i\}_{i=1}^{2}$, i.e. the maximal dimension given by theorem 1. Observe that $\tilde{k}_{ij} \geqslant 2$ and for adjacent sectors the inequality must be strict. Therefore it follows that the manifold dimension cannot be reduced via a degeneracy: e.g. attempt to remove the dependence on θ_1 by equating the coefficients of $\cos(4\theta_1)$ and $\cos\big(4(\theta_2 - \theta_1)\big)$ to zero. This forthwith implies that $\tilde{k}_{12} = 2$, a contradiction since any two sectors out of the three are contiguous. A similar contradiction ensues when any other pair of coefficients in (15a) enclosed in curly braces is let vanish.

Figure 4 depicts a typical cross-section of the singular manifold. Bearing in mind the limitation $0 \leqslant \theta_1 < \theta_2 < 2\pi$, for most values of θ_1 there are 4, 6 or 8 values of θ_2 that conform to a singular configuration (a vertical line intersects each petal-shaped contour twice, and the total number thereof includes the ones shown above the dotted line along with replicas within $\pi \leqslant \theta_2 \leqslant 2\pi$). Proposition 1 proves this is so for any combination of permeabilities. Therefore an arbitrarily chosen configuration is never far from a singular one and will manifest dynamics governed by a mechanism similar to that in lemma 1, as is proved hereinafter in theorem 2.

Nonetheless there exist "corridors" of both θ_1 and θ_2 such that for a fixed value of one, the configuration is non-singular for any value of the other. This happens when it is possible to draw a vertical or horizontal line on the (θ_1, θ_2) plane without intersecting any of the petal-shaped contours. In the example in figure 4 the horizontal regularity corridors are wider than the vertical ones. The asymmetry exists since (15) is not invariant under the reflexion mapping $\theta_1 \longleftrightarrow \theta_2$. Furthermore, these corridors grow narrower as the disparity in permeability values increases: the green contours leave little room to draw a line whilst avoiding all intersections. Figure 5 illustrates how the corridor width $\Delta\theta_1$ diminishes if one sector's permeability is gradually increased four orders of magnitude, opening a preferential direction of flow. Realistic permeability values naturally span such a range. The respective interval of θ_1, where no choice of the ray θ_2 will result in a singular configuration, quickly decreases two orders of magnitudes (the exemplary linearity of the log-log dependence is unlikely to be a generic feature and is a topic of future study). Therefore if a preferential flow direction exists, any given configuration is almost certainly close to a singular one, inducing the sensitivity of the flow field and in particular the boundaries of the zone of influence to small changes in geometry.

Proposition 1. *Let $N = 3$ and $\theta_3 = 2\pi$ without loss of generality. Then there exists exactly one horizontal and one vertical regularity corridor in any square representing one period of the manifold $m_n\pi/2 \leqslant \theta_n \leqslant (m_n+1)\pi/2$, $n = \{1,2\}$ and $m_n \geqslant 0$ an arbitrary integer.*

Proof. Rearrange equation (15a) to read

$$\sin\big(4(\theta_2+\beta)\big) = \frac{T_0 - T_1\cos(4\theta_1)}{\sqrt{T_2^2 + 2T_2T_{12}\cos(4\theta_1) + T_{12}^2}}, \tag{16a}$$

where

$$\tan(4\beta) = \frac{T_2 + T_{12}\cos(4\theta_1)}{T_{12}\sin(4\theta_1)} \tag{16b}$$

and

$$T_0 = \tilde{k}_{12}+\tilde{k}_{13}+\tilde{k}_{23}-6, \quad T_1 = \tilde{k}_{12}+\tilde{k}_{13}-\tilde{k}_{23}-2, \quad T_2 = -\tilde{k}_{12}+\tilde{k}_{13}+\tilde{k}_{23}-2, \quad T_{12} = \tilde{k}_{12}-\tilde{k}_{13}+\tilde{k}_{23}-2$$

are combinations of the coefficients $\tilde{k}_{ij}$ in (15b). The right-hand side of (16a) defines a function $f(\theta_1)$

$$f(\theta_1) = \frac{T_0 - T_1\cos(4\theta_1)}{\sqrt{T_2^2 + 2T_2T_{12}\cos(4\theta_1) + T_{12}^2}}, \tag{17}$$

and its values determine whether there is a solution $\theta_2(\theta_1)$. A range of θ_1 wherein $|f(\theta_1)| \leqslant 1$ produces the contours as in figure 4. A range where $|f(\theta_1)| > 1$ conforms to the regularity corridors.

Differentiating f and seeking extrema gives two options:

$$\sin(4\theta_1) = 0 \tag{18a}$$

and

$$\cos(4\theta_1) = -\frac{T_0}{T_1} - \frac{T_2}{T_{12}} - \frac{T_{12}}{T_2}. \tag{18b}$$

Limiting the values to one period, (18a) yields $\theta_1 = 0, \pi/4$. The values at these points are

$$f(0) = 1, \quad f\left(\frac{\pi}{4}\right) = \frac{\tilde{k}_{12}+\tilde{k}_{13}-4}{\left|\tilde{k}_{12}-\tilde{k}_{13}\right|}.$$

Since the values of K_n must be distinct in adjacent sectors, $\tilde{k}_{12} > 2$ and $\tilde{k}_{13} > 2$, whereby $f(\pi/4) > 1$ and in particular $f(\pi/4) = \infty$ if $\tilde{k}_{12} = \tilde{k}_{13}$. Suppose that (18b) has no roots. Bar the case $\tilde{k}_{12} = \tilde{k}_{13}$, continuity will imply that $\theta_1 = 0$ must be a minimum and $\theta_1 = \pi/4$ a maximum. This is impossible, as then $f(\theta_1) \geqslant 1 \ \forall 0 \leqslant \theta_1 \leqslant \pi/2$, and the dimension of the singular manifold is insufficient, as only point solutions θ_2 will ensue. Therefore one infers that the points $\theta_1 = 0$ and $\theta_1 = \pi/4$ are both maxima and (18b) must have roots. A trigonometric equation of this type will produce exactly 2 roots per period, and thus these must be minima of $f(\theta_1)$ located on two sides of $\pi/4$. For the case $\tilde{k}_{12} = \tilde{k}_{13}$ the maximum at $\pi/4$ becomes an asymptote, but $f(\theta_1) \longrightarrow \infty$ on both sides, so the analysis still holds. Thus between the two minima and the maximum at $\pi/4$ lie two points θ_{1c} such that $f(\theta_{1c}) = 1$. These delimit the only regularity corridor in any one period of θ_1 and are given by

$$T_1^2\cos^2(4\theta_{1c}) - 2\big(T_0T_1 + T_2T_{12}\big)\cos(4\theta_{1c}) + T_0^2 - T_2^2 - T_{12}^2 = 0 \tag{19}$$

upon discarding the roots at multiples of $\pi/2$.

To obtain the result for the regularity corridor of θ_2, swap $\theta_1 \longleftrightarrow \theta_2$ and $T_1 \longleftrightarrow T_2$. The analysis is identical, upon verification that $f(0) = 1$ and $f(\pi/4) > 1$ still hold. □

A typical graph of $f(\theta_1)$ corresponding to the manifold in figure 4 is shown in figure 6. From proposition 1 it forthwith follows that the regularity corridors are centred about $\pi/4$, regardless of permeability ratios, for both θ_1 and θ_2 (with $\pi/2$ periodic replicas). Bearing in mind that $\theta_3 = 2\pi$ and $\theta_2 > \theta_1$, but rotational translation is allowed, one infers that unless one sector is of an angle approximately $\pi/4$ or $3\pi/4$, most choices of angles for the remaining two sectors will result in a proximity to a singular configuration, and thus measurements of the zone of influence are expected to yield erratic results.

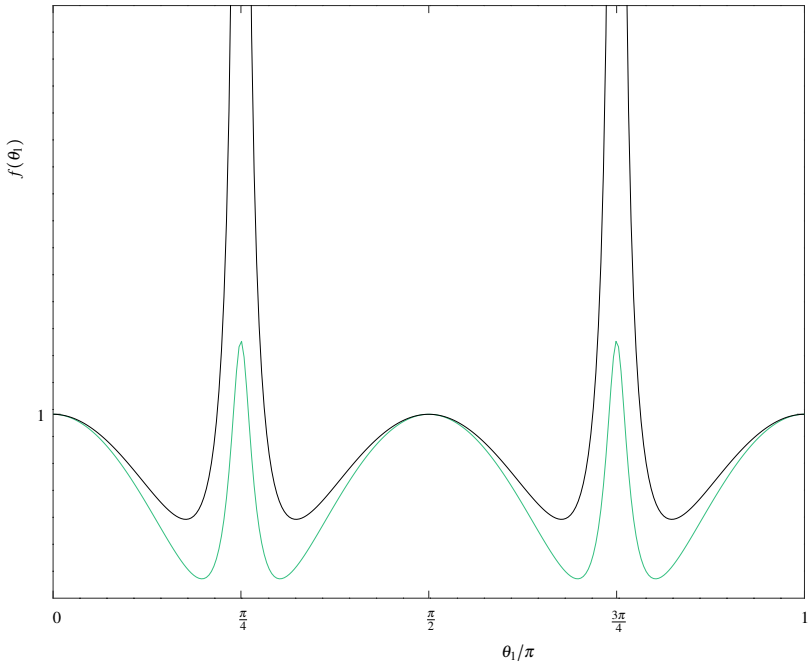

Figure 6. Regularity corridor function: equation (17) with parameters and colour scheme as in figure 4

2.3. $N = 4$

Without loss of generality set $\theta_4 = 2\pi$. Partition the matrix $\mathfrak{C}$ in (7c) into 4 square 4×4 blocks as follows:

$$\mathfrak{C} = \begin{pmatrix} \mathfrak{C}_1 & \mathfrak{C}_2 \\ \mathfrak{C}_3 & \mathfrak{C}_4 \end{pmatrix}$$

and multiply on the right by $\begin{pmatrix} \mathrm{I}_{4\times4} & 0_{4\times4} \\ -\mathfrak{C}_4^{-1}\mathfrak{C}_3 & \mathrm{I}_{4\times4} \end{pmatrix}$. Since $\mathfrak{C}_4$ is block diagonal, its inversion involves minimal effort. The resulting matrix is also block diagonal and requires to operate on 4×4 matrices to compute its determinant. The determinant of the auxiliary matrix is unity. Upon simplification the singular manifold $\det\mathfrak{C} = 0$ is given by

$$\begin{aligned}
&\cos(4\theta_1)\left\{\tilde{k}_{12}+\tilde{k}_{13}+\tilde{k}_{14}-\tilde{k}_{23}-\tilde{k}_{24}-\tilde{k}_{34}+\tilde{\tilde{k}}-2\right\}+\cos(4\theta_2)\left\{-\tilde{k}_{12}+\tilde{k}_{13}+\tilde{k}_{14}+\tilde{k}_{23}+\tilde{k}_{24}-\tilde{k}_{34}-\tilde{\tilde{k}}-2\right\}+\\
&\cos(4\theta_3)\left\{-\tilde{k}_{12}-\tilde{k}_{13}+\tilde{k}_{14}-\tilde{k}_{23}+\tilde{k}_{24}+\tilde{k}_{34}+\tilde{\tilde{k}}-2\right\}+\cos\big(4(\theta_2-\theta_1)\big)\left\{\tilde{k}_{12}-\tilde{k}_{13}-\tilde{k}_{14}+\tilde{k}_{23}+\tilde{k}_{24}-\tilde{k}_{34}+\tilde{\tilde{k}}-2\right\}+\\
&\cos\big(4(\theta_3-\theta_1)\big)\left\{\tilde{k}_{12}+\tilde{k}_{13}-\tilde{k}_{14}-\tilde{k}_{23}+\tilde{k}_{24}+\tilde{k}_{34}-\tilde{\tilde{k}}-2\right\}+\cos\big(4(\theta_3-\theta_2)\big)\left\{-\tilde{k}_{12}+\tilde{k}_{13}-\tilde{k}_{14}+\tilde{k}_{23}-\tilde{k}_{24}+\tilde{k}_{34}+\tilde{\tilde{k}}-2\right\}+\\
&\cos\big(4(\theta_3-\theta_2+\theta_1)\big)\left\{\tilde{k}_{12}-\tilde{k}_{13}+\tilde{k}_{14}+\tilde{k}_{23}-\tilde{k}_{24}+\tilde{k}_{34}-\tilde{\tilde{k}}-2\right\}=\tilde{k}_{12}+\tilde{k}_{13}+\tilde{k}_{14}+\tilde{k}_{23}+\tilde{k}_{24}+\tilde{k}_{34}+\tilde{\tilde{k}}-14,
\end{aligned} \tag{20a}$$

where k_{ij} are as in (15b) and

$$\tilde{\tilde{k}} = \frac{K_1K_3}{K_2K_4}+\frac{K_2K_4}{K_1K_3}. \tag{20b}$$

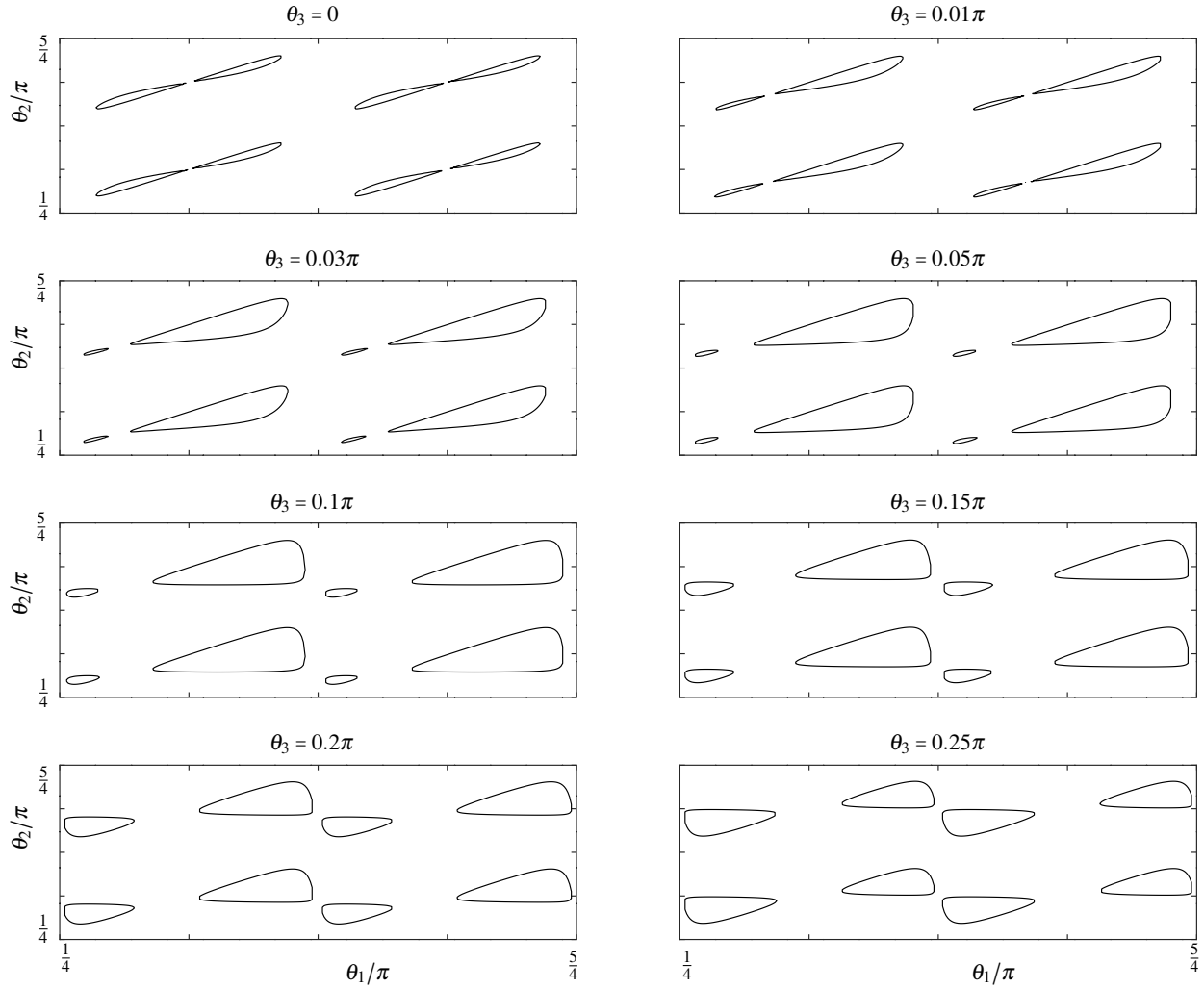

Figure 7. Singular manifold $\theta_2(\theta_1;\theta_3)$ by (20) with $k_1 = 0.1$, $k_2 = 20$, $k_3 = 5$

Including the fixed θ_4, this is a 6-dimensional manifold in the parameter space $\{\theta_n\}_{n=1}^4 \bigcup \{k_i\}_{i=1}^3$, the maximal dimension predicted by theorem 1. No degeneracy is possible. For instance, to remove the dependence on θ_1, four coefficients in curly braces in (20a) must vanish:

$$\begin{aligned}
\tilde{k}_{12} + \tilde{k}_{13} + \tilde{k}_{14} - \tilde{k}_{23} - \tilde{k}_{24} - \tilde{k}_{34} + \tilde{\tilde{k}} - 2 = 0,\\
\tilde{k}_{12} - \tilde{k}_{13} - \tilde{k}_{14} + \tilde{k}_{23} + \tilde{k}_{24} - \tilde{k}_{34} + \tilde{\tilde{k}} - 2 = 0,\\
\tilde{k}_{12} + \tilde{k}_{13} - \tilde{k}_{14} - \tilde{k}_{23} + \tilde{k}_{24} + \tilde{k}_{34} - \tilde{\tilde{k}} - 2 = 0,\\
\tilde{k}_{12} - \tilde{k}_{13} + \tilde{k}_{14} + \tilde{k}_{23} - \tilde{k}_{24} + \tilde{k}_{34} - \tilde{\tilde{k}} - 2 = 0.
\end{aligned}$$

Summing the first and second pairs, and then summing the resulting equations yields $\tilde{k}_{12} = 2$, a contradiction, since for adjacent sectors $\tilde{k}_{ij} > 2$. A similar process rules out a lesser dimension via the removal of the dependence on θ_2 or θ_3.

Figure 7 depicts an example of this manifold as 8 cross-sections of θ_3. This time the petal-shaped loci shift and change size asymmetrically, so the regularity corridors are tunnels of non-uniform cross-section and orientation. Therefore any realistic configuration is always close to a singular one, giving rise to erratic results when the zone of influence is probed in the field. Theorem 2 proves this result for an arbitrary configuration.

2.4. Arbitrary N

Although a certain structure of the singular manifold does emerge from the comparison of the first two non-degenerate cases (15) and (20), generalising to an arbitrary number of sectors appears convoluted. Nevertheless the $\pi/2$ periodicity in all θ_n must hold. It can only be conjectured that the actual dimension $2(N-1)$ will remain non-degenerate. An elegant implicit expression for the manifold can be obtained via an LU decomposition of $\mathfrak{C}$:

$$\mathfrak{C} = \begin{pmatrix} \mathrm{I}_{2\times2} & & & & \\ \mathrm{L}_{21} & \mathrm{I}_{2\times2} & & & \\ & \ddots & \ddots & & \\ & & & \mathrm{I}_{2\times2} & \\ \mathrm{L}_{N1} & & & \mathrm{L}_{N,N-1} & \mathrm{I}_{2\times2} \end{pmatrix} \begin{pmatrix} \mathfrak{A}_1 & \mathfrak{B}_1 & & & \\ & \mathfrak{A}_2 & \mathfrak{B}_2 & & \\ & \ddots & \ddots & & \\ & & & \mathfrak{A}_{N-1} & \mathfrak{B}_{N-1} \\ & & & & \mathrm{U}_{NN} \end{pmatrix}, \tag{21a}$$

where $\mathfrak{A}_n$, $\mathfrak{B}_n$ are defined beneath (7c) and

$$\mathrm{U}_{NN} = \mathfrak{A}_N - (-1)^N \mathfrak{B}_N \mathfrak{A}_1 \mathfrak{B}_1 \times \ldots \times \mathfrak{A}_{N-1} \mathfrak{B}_{N-1}. \tag{21b}$$

Since the determinant of the lower triangular matrix is unity and all blocks $\mathfrak{A}_n$, $\mathfrak{B}_n$ are invertible, it follows that

$$\det \mathfrak{C} = (-1)^N \det\Big(\mathrm{I}_{2\times2} - (-1)^N \mathfrak{A}_1 \mathfrak{B}_1 \times \ldots \times \mathfrak{A}_N \mathfrak{B}_N\Big). \tag{22}$$

The precise shape of the singular manifold is required in order to differentiate between mathematically singular and non-singular configurations. However, in practice this binary distinction is not particularly helpful, since a proximity to a singularity suffices to induce structural inconsistencies in the underlying flow field. The following theorem generalises lemma 1 to an arbitrary number of sectors and constitutes the salient conceptual argument in support of the claim that the erratic zone of influence sampling results are in fact inherent to the weakly compressible flow through a heterogeneous porous medium.

Theorem 2. *Let N be the number of sectors. Without loss of generality the functions*

$$p_n^2 = \frac{C_n}{2K_n}\left\{ {b_1}_0^{(n)} + \frac{1}{2} {b_2}_0^{(n)} \ln\big(x^2+y^2\big) + 2{a_1}_2^{(n)} xy + \big({b_1}_2^{(n)} - 1\big)x^2 - \big({b_1}_2^{(n)} + 1\big)y^2 \right\}$$

conform to solution (6) with no harmonics of $m > 2$, coefficients $b_{i_0}^{(n)}$ given by (9c) – (9d) and coefficients ${a_1}_2^{(n)}$, ${b_1}_2^{(n)}$ as in (7c). Further let $\bar{\theta}_o$ define a N-tuple of contiguity rays such that system (7c) is singular, i.e. $\det \mathfrak{C}(\bar{\theta}_o) = 0$. Further let $\bar{\theta} = \bar{\theta}_o + \varepsilon\bar{\theta}_1$ with $\bar{\theta}_1 \sim \mathcal{O}(1)$ and $|\varepsilon| \ll 1$ define a configuration that is a small perturbation of the singular one. Then in the respective flow field
(i) if critical points exist, they are saddle points;
(ii) there are at most two such points in any given sector;
(iii) when ε changes sign, said saddle points either shift abruptly by an angle of $\pi/2$ or disappear.

Proof. If existing, the critical points (r_*, θ_*) solve

$$\frac{{b_2}_0^{(n)}}{r_*} + 2r_*\Big(-1 + {a_1}_2^{(n)} \sin(2\theta_*) + {b_1}_2^{(n)} \cos(2\theta_*)\Big) = 0, \tag{23a}$$

$${a_1}_2^{(n)} \cos(2\theta_*) - {b_1}_2^{(n)} \sin(2\theta_*) = 0. \tag{23b}$$

As the attention is on a specific sector where such points might exist, the superscripts might be omitted. To verify the nature of these points, compute the second order partial derivatives and use (23b) to obtain

$$p_{xx}(r_*, \theta_*) = \frac{2}{p}\Big(b_{12} - \cos^2\theta_*\Big), \tag{24a}$$

$$p_{yy}(r_*,\theta_*) = -\frac{2}{p}\Big(b_{12}+\sin^2\theta_*\Big) \tag{24b}$$

and

$$p_{xy}(r_*,\theta_*) = \frac{1}{p}\Big(2a_{12}-\sin(2\theta_*)\Big). \tag{24c}$$

The Hessian matrix determinant is then

$$\det\mathfrak{H} = p_{xx}p_{yy}-p_{xy}^2 = -\frac{4}{p^2}\Big(a_{12}^2+b_{12}^2-b_{12}\cos(2\theta_*)-a_{12}\sin(2\theta_*)\Big). \tag{25a}$$

By (23b) if $b_{12}\neq 0$, $\tan(2\theta_*) = a_{12}\Big/b_{12}$. Then by the identity $1+\tan^2(2\theta_*) = \csc^2(2\theta_*)$

$$\cos(2\theta_*) = \pm\,\frac{b_{12}}{\sqrt{a_{12}^2+b_{12}^2}}, \qquad \sin(2\theta_*) = \pm\,\frac{a_{12}}{\sqrt{a_{12}^2+b_{12}^2}},$$

where the plus and minus signs must be respective, as cross-matching will contradict (23b). This allows to re-write (25a) as

$$\det\mathfrak{H} = -\frac{4}{p^2}\sqrt{a_{12}^2+b_{12}^2}\left(\sqrt{a_{12}^2+b_{12}^2}\pm 1\right). \tag{25b}$$

If $b_{12}=0$, by (23b) $\cos(2\theta_*)=0$ since $a_{12}\neq 0$, as is to be shown forthwith. Then $\sin^2(2\theta_*)=1$ and (25b) in fact includes this as a particular case. Thus if $a_{12}^2+b_{12}^2>1$, $\det\mathfrak{H}<0$ for all values of a_{12}, b_{12}, and the critical point must be a saddle point. To see that it is impossible to have $a_{12}=b_{12}=0$ in any sector, observe that system (7c) comprises $N-1$ block equations of the form

$$\mathfrak{A}_n\bar{c}_n+\mathfrak{B}_n\bar{c}_{n+1}=\bar{r}_n, \quad 1\leqslant n<N \tag{26a}$$

and one block of the form

$$\mathfrak{B}_1\bar{c}_1+\mathfrak{B}_N\bar{c}_N=\bar{r}_N, \tag{26b}$$

where

$$\bar{c}_n = \begin{pmatrix} a_{12}^{(n)} \\ b_{12}^{(n)} \end{pmatrix}, \quad \bar{r}_n = \begin{pmatrix} 1-k_n \\ 0 \end{pmatrix}, \qquad 1\leqslant n\leqslant N.$$

Suppose $\bar{c}_{n_*}=\bar{0}$ for some $1<n_*<N$. Block n_* in (26a) will immediately yield $\bar{c}_{n_*+1}$ and subsequent blocks will give all $\bar{c}_n$ for $n_*+2\leqslant n\leqslant N$. Block n_*-1 in (26a) will yield $\bar{c}_{n_*-1}$ and similarly blocks 1 to n_*-2 will give all remaining $\bar{c}_n$, $1\leqslant n\leqslant n_*-2$. Then block (26b) renders the system overdetermined and becomes a contradiction. An identical argument follows for $n_*=1$ or $n_*=N$ with (26a) solved block by block in a single sequence going either forwards or backwards instead of both. Thus at least one of the coefficients a_{12}, b_{12} in any sector must be non-zero.

The next step is to show that at least one out of a_{12}, b_{12} exceeds unity in magnitude. For a configuration that is a small perturbation of the singular one system (7c) can be written as

$$\mathfrak{C}\mathbf{c} = \Big(\mathfrak{C}_o+\varepsilon\mathfrak{C}_1+\mathcal{O}\big(\varepsilon^2\big)\Big)\mathbf{c} = \mathbf{r}, \tag{27}$$

where $\mathfrak{C}_o = \mathfrak{C}(\bar{\theta}_o)$ is singular and $\mathfrak{C}_1 = \dfrac{\mathrm{d}\mathfrak{C}_o}{\mathrm{d}\theta}\bigg|_{\bar{\theta}_o}$. By Cramer's rule the n-th entry of $\mathbf{c}$ is given by

$$c^{(n)} = \frac{\det\tilde{\mathfrak{C}}_n}{\det\mathfrak{C}}, \tag{28}$$

where $\tilde{\mathfrak{C}}_n$ is the matrix $\mathfrak{C}$ with column n replaced by $\mathbf{r}$. Similarly to the computation of the characteristic polynomial, $\det\Big(\mathfrak{C}_o+\varepsilon\mathfrak{C}_1+\mathcal{O}\big(\varepsilon^2\big)\Big)$ will be a polynomial of order $2N$ in entries from $\varepsilon\mathfrak{C}_1+\mathcal{O}\big(\varepsilon^2\big)$, i.e. a power series in ε.

However, since $\lim_{\varepsilon \longrightarrow 0} \det \mathfrak{C} = \det \mathfrak{C}_o = 0$, the free coefficient of the limit polynomial vanishes, whereas $\lim_{\varepsilon \longrightarrow 0} \det \tilde{\mathfrak{C}}_n \neq 0$, giving a power series with a non-zero free coefficient. Therefore

$$c^{(n)} \sim \mathcal{O}\left(\varepsilon^{-1}\right). \tag{29}$$

Thus as $\varepsilon \longrightarrow 0$, any non-vanishing coefficients a_{12}, b_{12} exceed unity in magnitude and hence any critical point must be a saddle point.

By (23b) the angle θ_* is

$$\theta_* = \frac{1}{2}\left(\arctan\frac{a_{12}}{b_{12}} + \pi m\right), \tag{30}$$

where different values of the integer m must give distinct solutions within the same sector. Thus if the saddle point "skips", it can only be by an angle of $\pi/2$ or π (clockwise or counter-clockwise). By (23a)

$$2r_*^2 = \frac{b_{20}}{1 - a_{12}\sec(2\theta_*)} \tag{31a}$$

if $\sin(2\theta_*) \neq 0$, and

$$2r_*^2 = \frac{b_{20}}{1 - b_{12}\csc(2\theta_*)} \tag{31b}$$

if $\cos(2\theta_*) \neq 0$. At the limit $\varepsilon \longrightarrow 0$ the estimate (29) respectively implies

$$r_*^2 \sim \text{const} \cdot \cos(2\theta_*)\,\varepsilon + \mathcal{O}\left(\varepsilon^2\right), \qquad \sin(2\theta_*) \neq 0, \tag{32a}$$

$$r_*^2 \sim \text{const} \cdot \sin(2\theta_*)\,\varepsilon + \mathcal{O}\left(\varepsilon^2\right), \qquad \cos(2\theta_*) \neq 0. \tag{32b}$$

Therefore if ε changes sign, the saddle point must shift its location abruptly because $r_*^2 > 0$. A skip of π does not alter the sign of $\sin(2\theta_*)$ and $\cos(2\theta_*)$, but implies that if that skip falls within the same sector, there must be two saddle points and no more. Thus either the angle $\theta_* \pm \pi/2$ puts the point within the same sector, begetting the required shift, or the new angle is outside the sector, and the saddle point will disappear. Either possibility does not bar appearance of new saddle points in other sectors. □

Figure 8 illustrates this behaviour for $N = 3$. Note that in panel (a) there is a single saddle point in sectors 2 and 3. In panel (b) ε changed sign, causing the point in sector 2 to disappear because an angle skip of $\pi/2$ would place it outside its sector, whereas the point in sector 3 follows through with the required shift, morphing into two points located on a perpendicular line.

The main practical inference to be made from theorem 2 is that the abrupt shifting of the saddle points in the vicinity of a singular configuration is the generic behaviour. The exposition on the frequency of occurrence of singular configurations compels the conclusion that a given configuration of a specific well site is very likely to fall close to a singular one. In conjunction with the understanding that disparity in permeability ratios of the different sectors will beget critical points, even small fluctuations in the sectors' angles will induce rapid transitions of pressure and streamlines between acutely differing steady states. This establishes the theoretical basis for the strong fluctuations routinely encountered in the field. The critical points of the pressure field correspond to flow stagnation points as well as the farthest points of the separatrix pressure contour that delineates the zone of influence within each sector. A sudden rearrangement of these points causes a disruption in the flow field and thus ineffective well function.

3. Discussion

Locally radial flow from or toward a well of a weakly compressible fluid through a porous medium underpins efficient performance of numerous environmental engineering applications from aquifer sparging to landfill gas and natural gas extraction. The zone of influence of such a well has traditionally been described by a single scalar referred to

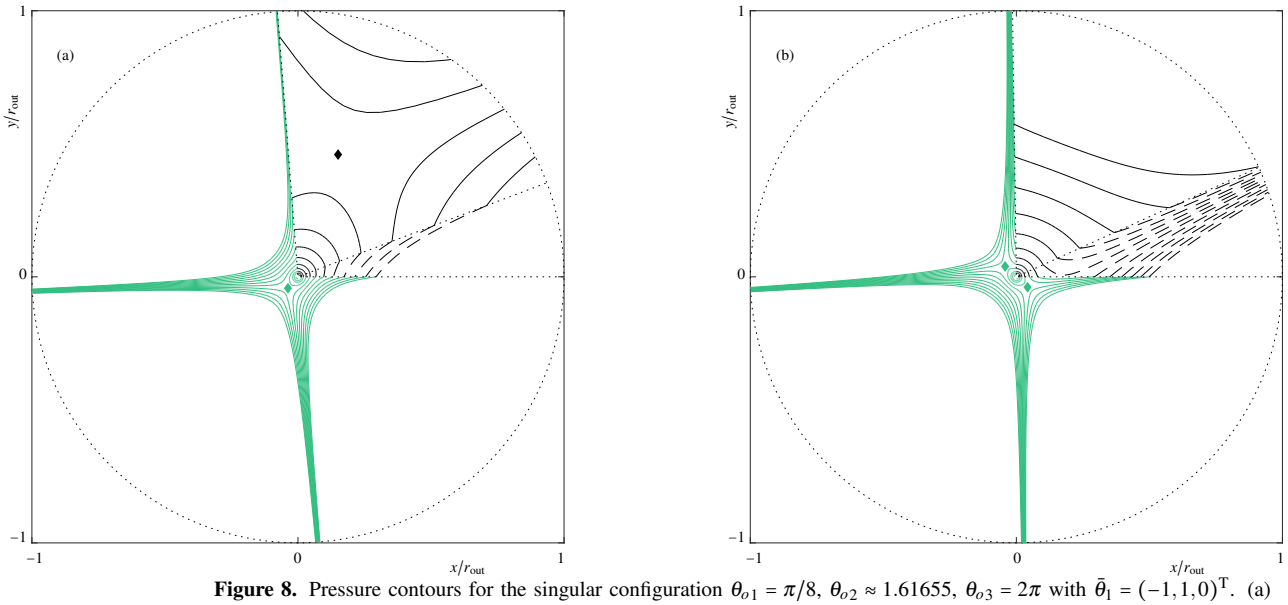

Figure 8. Pressure contours for the singular configuration $\theta_{o1} = \pi/8$, $\theta_{o2} \approx 1.61655$, $\theta_{o3} = 2\pi$ with $\bar{\theta}_1 = (-1, 1, 0)^{\mathrm{T}}$. (a) $\varepsilon = 0.01\pi$, (b) $\varepsilon = -0.01\pi$. $k_1 = 0.1$, $k_2 = 100$. Diamonds mark saddle points.

as a radius, adopted from the field of hydraulic wells, where it also enjoys some controversy (Bresciani et al., 2020). For want of a better alternative, this concept is predominant despite long-standing and well documented difficulties in measuring or even defining the radius of influence in practice. Most practical definitions select a threshold that is often chosen *after* the data are collected and cleaned, be they field measurements or computational results: a certain head loss that is deemed undetectable and usually depends on the instrumentation employed; or an arbitrary drop in the concentration of dissolved oxygen; or in numerical simulations a given number of orders of magnitude that the radial velocity (proportional to the gradient of pressure) must diminish relative to the value at the well before the collection of fluid or dispersion of injected fluid is considered ineffectual. Whilst any individual choice might be well substantiated, collectively the ambivalence is staggering. The struggle to define and quantify the radius of influence makes it abundantly clear there must be an essential flaw in this concept as applied to this type of flow.

Whilst the dependence of a well's reach on depth figured in both experimental and numerical studies, one aspect that has been consistently overlooked is the possible azimuthal dependence. The wide class of exact flow solutions with azimuthally discontinuous permeability accords an explanation of the difficulty to measure or predict the radius of influence accurately from a unique vantage point. The natural terrain around an aquifer or natural gas deposit, as well as the man-made landfill medium, is heterogeneous, at times highly so. There are preferential directions of flow due to differences in the matrix saturation or density. These can be relatively large sectors, such as a rock massif or highly compacted waste cell, or constitute no more than a sliver of a less resistant medium, as in hydraulic fracturing. This solution class encompasses all of the foregoing situations and harbours two mathematical properties that translate directly into the inability to attain a well-posed description of the radius of influence.

One, the broken axial symmetry begets a zone of influence that cannot be captured by a single scalar, as the contours are no longer concentric circles, but oblate shapes with non-smooth boundaries. This feature compels an adjustment of the classical notion of a radius into a range delimited by the farthest and nearest points on the largest closed (separatrix) contour. The azimuthal variation accounts for the large errors – tens to hundreds of per cent – observed when the monitoring points are not situated on a straight ray emanating from the well centre.

The second property elucidates the abrupt and defying all conventional modelling temporal changes. These have been correctly attributed to fluctuations in medium permeability due to saturation or similar natural qualitative variation outside of the well operators' control and only detectable with the aid of advanced tri-dimensional imaging. The foregoing class of solutions is heavily ridden with singularities, formally expressed via the co-dimension of the singular manifold within the parameter space. The preliminary physical parameter space has dimension $3N$ with N being the number of sectors of distinct permeabilities and/or generation rates. When these are grouped into ratios, the effective dimension is $d_{\text{eff}} = 3N - 2$. For any $N > 2$ the co-dimension of the singular manifold is $d_{\text{sing}} = 2(N-1)$. For $N = 2$ the manifold is degenerate with a co-dimension of unity. It follows that for any $N > 2$ the dimension of the singular manifold always exceeds that of its regular complement $d_{\text{reg}} = 3N - 2 - 2(N-1) = N$, since $2(N-1) > N$. If some of the sectors possess the same generation rate, the dimension of the regular subspace is further reduced, as d_{eff} diminishes, whilst d_{sing} remains fixed, because the generation rates do not participate in the structural mechanism responsible for the formation of the singular manifold. In the most extreme, but realistically likely, case of an equal generation rate throughout the domain, $d_{\text{eff}} = 2N$, $d_{\text{sing}} = 2(N-1)$, whilst $d_{\text{reg}} = 2$. In reality the flow field in a domain corresponding to a singular configuration would be unsteady. The disparity of the steady flow fields in the vicinity of a singularity determine the severity of the required transition. Herein it was shown that the change is indeed momentous – stagnation points shift to a perpendicular line and/or appear or disappear. As the separatrix contour defining the zone of influence must pass through these points, the abruptness of the ensuing adjustment explains the inconsistence encountered whilst attempting to measure descriptive flow parameters such as pressure or solute concentration that bear on the zone of influence.

For a low number of sectors $3 \leqslant N \leqslant 4$ it was shown explicitly that most configurations are never far from a singular one. Whilst regularity tunnels do exist, they are narrow and permeability dependent. Fast permeability fluctuations caused by such factors as water table, leachate levels etc. might easily cause a transition through a singular configuration, engendering a qualitative change in pressure contours and gradients, location of stagnation points and consequently the shape and orientation of the contour delimiting the zone of influence.

To conclude, the weakly compressible flow in a porous medium with azimuthally discontinuous permeability is a fascinating dynamical system with a complex pattern of singularities, whose most notable feature is a pronounced shift in the flow characteristics in the vicinity thereof. This quality was used to interpret the enduring difficulty to measure and predict the radius of influence of wells in environmental engineering applications as an intrinsic peculiarity of the weakly compressible flow in an anisotropic porous medium. It was shown that a more adequate description would be a zone of influence, whose azimuthal dependence is considered in field studies.

References

Agarwal N, Semmens M J, Novak P J and Hozalski R M 2005 *Water Resour. Res.* **41**, W05017.
Al-Hussainy R, Jr. H J R and Crawford P B 1966 *J. Pet. Technol.* **18(05)**, 624–636.
Bresciani E, Shandilya R N, Kang P K and Lee S 2020 *J. Hydrol.* **583**, 124646.
Freedman V L, Mackley R, Waichler S R and Horner J 2013 *J. Hydrol. Eng.* **18(9)**, 1170–1179.
Fulks W B, Guenther R B and Roetman E L 1971 *Acta Mech.* **12**, 121–129.
Germanou L, Ho M T, Zhang Y and Wu L 2018 *J. Nat. Gas Sci. Eng.* **60**, 271–283.
Hyman J D, Karra S, Makedonska N, Gable C W, Painter S L and Viswanathan H S 2015 *Comp. Geosci.* **84**, 10–19.
Kutsyi D V 2015 *Therm. Eng.* **62(7)**, 495–502.
Li T, Ki M, Jing X, Xiao W and Cui Q 2019 *Pet. Explor. Dev.* **46(3)**, 594–604.
Li X, Lu D, Luo R, Sun Y, Shen W, Hu Y, Liu X, Qi Y, Guan C and Guo H 2019 *Pet. Explor. Dev.* **46(5)**, 998–1005.
Lundegard P D and LaBrecque D 1995 *J. Contam. Hydrol.* **19**, 1–27.
Mair R W, Wong G P, Hoffmann D, Hürlimann M D, Patz S, Schwartz L M and Walsworth R L 1999 *Phys. Rev. Lett.* **83**, 3324.
Mauran S, Rigaud L and Coudevylle O 2001 *Transp. Porous Media* **43**, 355–376.
Nec Y and Huculak G 2019 *Transp. Porous Media* **130(3)**, 769–797.
Nec Y and Huculak G 2020 *Phys. Fluids* **32**, 077108.
Stenborg J W and Williams D B 1994 *US Patent* **5295763**.
Vigneault H, Lefebvre R and Nastev M 2004 *Vadose Zone J.* **3**, 909–916.
Walter G R 2003 *J. Air Waste Manage. Assoc.* **53(4)**, 461–468.
Whitaker S 1986 *Transp. Porous Media* **1**, 3–25.
Young A 1989 *J. Environ. Eng.* **115(6)**, 1073–1087.